ACS APPLIED POLYMER MATERIALS

pubs.acs.org/acsapm

Article

Optimization of the Thermoelectric Properties of 2D-PEDOT Derivative Chains Using Electrochemical Control

Jun Seop Lee and Shrayesh N. Patel*

Cite This: ACS Appl. Polym. Mater. 2022, 4, 6978−6984

Read Online

ACCESS | Metrics & More | Article Recommendations | Supporting Information

ABSTRACT: Conductive organic-based thermoelectric generators are very effective in collecting electricity from waste heat with low-temperature gradients compared to ambient conditions. Although studies have been conducted to improve thermoelectric characteristics by doping conducting polymers, the thermoelectric performances achieved by accurately controlling the doping level of polymer chains are currently inadequate. Here, we report changes in thermoelectric performance of three-armed cross-linker introduced poly(3,4-ethylenedioxythiophene) (PEDOT) derivative two-dimensional (2D) chain using electrochemical oxidation level control. The charge carrier density of PEDOT derivative films increased with more positive potentials (from 0.7×10^{20} to 4.24×10^{21}) and was precisely controlled by varying potentials. Thermoelectric properties such as electrical conductivity, carrier mobility, and Seebeck coefficients were also manipulated through the application of different potentials. The power factor of the PEDOT derivative 2D chain was improved to 72.6 μW m^{-1} K^{-2} at +0.6 V, which was much higher than that of a neutral state at −1.4 V (5.1×10^{-2} μW m^{-1} K^{-2}).

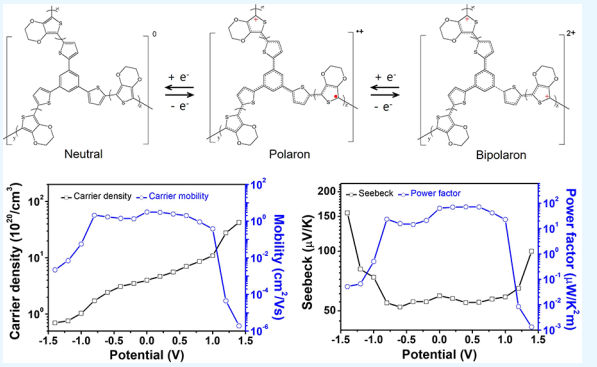

KEYWORDS: *organic thermoelectric, poly(3,4-ethylenedioxythiophene), doping control, electrical conductivity, Seebeck coefficient*

INTRODUCTION

Fossil fuels are currently the primary energy source for meeting most of society's demands for electricity. However, the carbon dioxide generated using fossil fuels is an important contributor to global warming. Therefore, an urgent need exists for alternative technologies that can increase the conversion efficiency of fossil fuels used for generating electricity or, alternatively, to produce electricity without them. Among the alternatives, thermoelectric generation (TEG) is an attractive technology due to its ability to generate power using industrial waste heat *via* the Seebeck effect.[1−3] The Seebeck effect can convert temperature differences directly into electrical voltages and is an important element of thermoelectric (TE) materials.[4−6] The efficiency of TE materials is expressed as the figure of merit $ZT = S^2\sigma T/\kappa$, where S is the Seebeck coefficient, σ is the electrical conductivity, κ is the thermal conductivity, and T is the absolute temperature.[7−9] From this definition, TE materials have to show large values for S and σ, with low κ, at low temperatures.[10−12] However, there are insufficient thermoelectric materials composed of high natural abundance elements that can work in the low-temperature region (<250 °C).[13−15] This limitation has triggered studies on conducting polymers as TE materials. These conducting polymers are relatively less expensive than inorganic materials because of the natural abundance of their component atoms and low toxicities.[16,17] Furthermore, these conducting polymers are easy to use in TEG devices as they utilize a solution process and a low-temperature annealing step.[18−20]

To improve the performance of a thermoelectric material, the three parameters (S, σ, and κ) which constitute ZT need to be simultaneously adjusted. As noted, κ as the denominator should have a small value ranging from 0.1 to 0.6 W m^{-1} K^{-1}.[21−23] In this regard, conducting polymers have sufficiently small κ values. However, with inorganic semiconductors, complex approaches are required to have small κ values.[24−26] Therefore, in research using conducting polymers as TE materials, the oxidation level of the polymer chain can be controlled to obtain a high power factor (PF) ($S^2\sigma$) value. The electrical conductivity (σ) and the Seebeck coefficient (S) as elements constituting the power factor have opposite aspects. That is, the value of σ increases in the high oxidation state, while the S decreases. Thus, to achieve high thermoelectric performance with conducting polymers, it is necessary to precisely control the oxidation level of the polymer chain and to find oxidation conditions in a specific state where PF is

Received: May 27, 2022
Accepted: September 7, 2022
Published: September 14, 2022

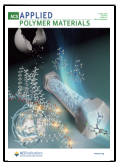

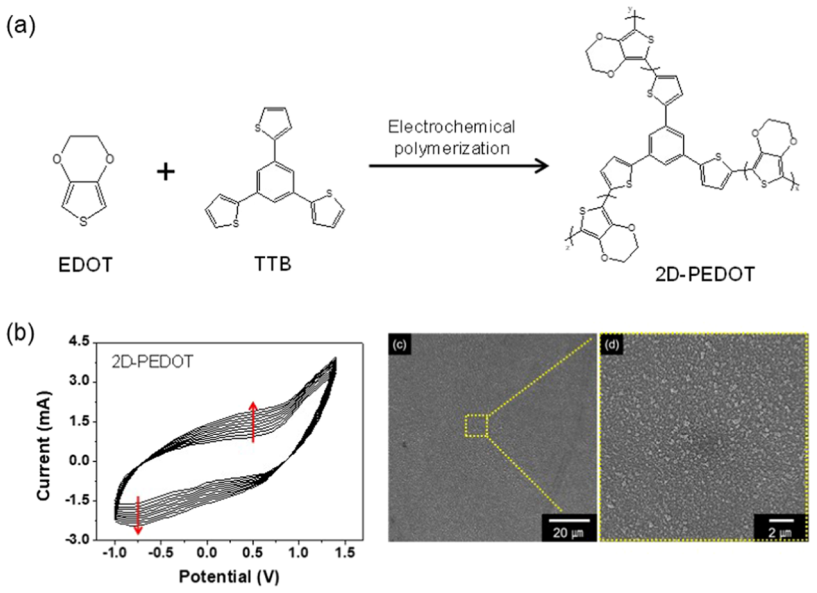

Figure 1. (a) Chemical structure changes after copolymerization of EDOT and TTB. (b) Ten-cycle CV curves of 2D-PEDOT during electrochemical polymerization. (c) Low- and (d) high-resolution FE-SEM images of the 2D-PEDOT film.

maximized. One approach to optimizing PF is to control redox states using molecular doping methods such as sequential doping, co-processing, and ion-exchange doping.[27−32] Among the three methods, sequential doping and ion-exchange doping have the advantage of obtaining high electrical conductivity without modifying the structure of the conducting polymer film. However, these methods are limited in use in areas where accurate doping amounts must be accurately controlled. In addition, the calculation of the oxidation level of these methods is not simple, and the type of counter ion is limited. On the other hand, an electrochemical doping method can better control the oxidation level of the conducting polymer by tuning the electrode potential and measuring the charging current.[33,34] In addition, abundant counter ions are present in this method to balance doping charges along the polymer chain using different salts in the electrolyte.

Herein, we report the optimization of the thermoelectric properties of a three-armed cross-linker introduced poly(3,4-ethylenedioxythiophene) (PEDOT) derivative two-dimensional chain (2D-PEDOT) through a facile electrochemical doping method. The 2D-PEDOT chain was synthesized using electropolymerization of 3,4-ethylenedioxythiophene (EDOT) and conjugated three-armed cross-linker (1,3,5-tri(2-thienyl)-benzene (TTB)). A small amount of TTB is covalently bonded with PEDOT to form a 2D-PEDOT chain, and this structure has superior electrical performance to conventional PEDOT chain structures. By simply controlling the oxidation process by varying the voltages of electrochemical cells, the thermoelectric properties of the 2D-PEDOT are changed by transforming the chemical structure of the polymer chain. To modify this process for thermoelectric application, the influence of the oxidation level on σ and S was systematically investigated and analyzed. Carrier density and mobility with different oxidation levels were also investigated to confirm the chemical structure changes of polymer chains.

RESULTS AND DISCUSSION

Synthesis of the 2D-PEDOT Chain. The poly(3,4-ethylenedioxythiophene) derivative 2D chain (2D-PEDOT) structure composed of 3,4-ethylenedioxythiophene (EDOT) and 1,3,5-tri(2-thienyl)-benzene (TTB) was synthesized using an electrochemical polymerization process (Figure 1a). Specifically, cyclic voltammetry (CV) scanning was performed over an optimized potential range (from −1 to +1.4 V) using a three-electrode system which included an indium tin oxide (ITO)/poly(ethylene terephthalate) (PET) film as a working electrode, a reference electrode of Ag/AgCl, and a counter electrode of Pt (Figure S1). In particular, the potential range for synthesis was set to include the oxidation potential of the two monomers (+0.8 V for TTB and +1.25 V for EDOT). To form a two-dimensional PEDOT chain structure, EDOT and TTB were added to the electrolyte at 10 and 0.5 mM, respectively. In this reaction, the TTB molecule must form a covalent bond with the PEDOT chain to form a polymer structure in the film. However, if TTB is added in excess to the electrolyte solution, TTB itself causes a polymerization reaction, forming different polymer structures. Based on electrochemical impedance spectroscopy (EIS) of the film according to TTB concentration, it was shown that one polymer chain exists at 0.5 mM or less, but two different polymer chains are created at concentrations greater than 0.5 mM (Figure S2). Figure 1b shows the CV curve of a 2D-PEDOT film after undergoing an electrochemical reaction ten times at a scan rate of 100 mV s^{-1}. The area of the CV curve increased as the number of reactions increased, indicating that polymer films were continuously generated. The CV curve of 2D-PEDOT had a different shape from films consisting of EDOT (PEDOT) or TTB (poly-TTB) only (Figure S3). For electrodes composed of TTB only, significant peaks did not appear except for redox peaks shown at +0.8 and +0.2 V. In addition, the CV curve of the 2D-PEDOT film showed a shape similar to that of the PEDOT film, although it had a larger area. Thus, synthesized 2D-PEDOT formed a polymer chain structure composed of TTB and EDOT. Moreover, field emission scanning electron microscopy (FE-SEM) of 2D-PEDOT showed a smooth surface with a uniform grain size (*ca.* 300 nm) (Figure 1c,d). These results confirmed that a

https://doi.org/10.1021/acsapm.2c00899
ACS Appl. Polym. Mater. 2022, 4, 6978−6984

small amount of TTB formed a uniform polymer chain structure with EDOT.

Chemical Property Changes of the 2D-PEDOT Chain. A three-electrode electrochemical process was used to measure performance changes according to the change in the oxidation level of synthesized 2D-PEDOT films (Figure 2). Specifically,

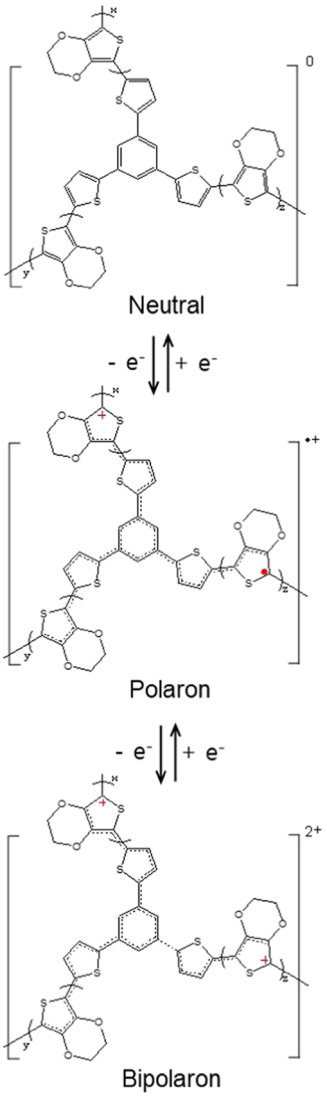

Figure 2. Chemical structures of 2D-PEDOT chains with different chemical states.

various voltages (from −1.4 to +1.4 V) were applied using the 2D-PEDOT film as a working electrode. After oxidizing, the polymer films were disconnected from the potentiostat, washed with isopropyl alcohol (IPA), and dried at 60 °C for 3 h in a nitrogen atmosphere to measure chemical, optical, and thermoelectric performance changes.

Fourier-transform infrared (FTIR) spectra were used to analyze the structure and vibration bond changes of the 2D-PEDOT film. Figure 3a shows the spectra generated (1850−600 cm^{-1}) by transforming the oxidation level of 2D-PEDOT films from −1 to +1 V. The FTIR spectra of the 2D-PEDOT film showed peaks originating from PEDOT chains. The band *ca.* 1520 cm^{-1} was caused by asymmetric C═C extending in the thiophene ring, and the symmetric C═C stretching vibration was generated *ca.* 1420 cm^{-1}.[27] Wide and weak band

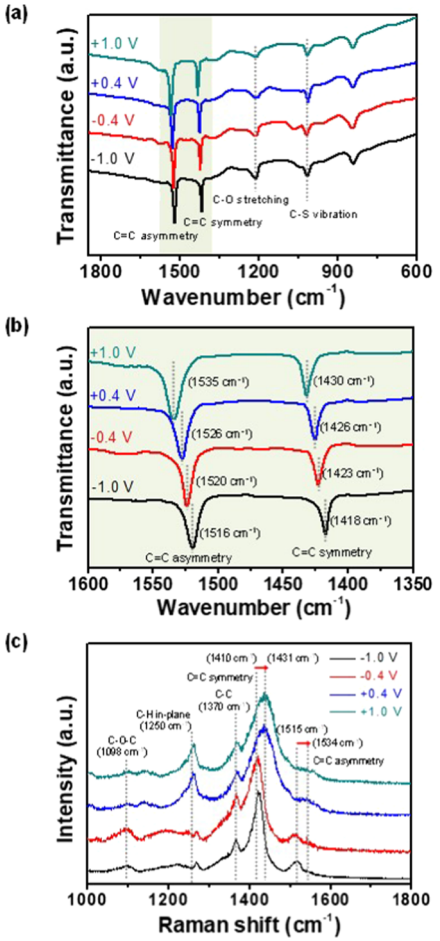

Figure 3. (a) Wide (1850−600 cm^{-1}) and (b) limited wavenumber area (1600−1350 cm^{-1}) of Fourier-transform infrared (FTIR) spectra and (c) Raman spectra of 2D-PEDOT with different applied potentials (black: −1.0 V, red: −0.4 V, blue: 0.4 V, and green: 1.0 V).

center *ca.* 1370 $cm^{-1}$was due to C−C ring stretching. The vibration *ca.* 1200 cm^{-1} was due to the C−O stretching mode of the ethylenedioxy group. The 980 cm^{-1} band represented the C−S vibrating bond of the thiophene ring. However, oxidation of the 2D-PEDOT film shifted asymmetric and symmetric C═C bonds of the chain (Figure 3b). Positions of C═C asymmetric and C═C symmetric peaks changed (1516−1535 cm^{-1} for C═C asymmetric and 1418−1430 cm^{-1} for C═C symmetric) due to conversion of the polymer chain from quinoid to benzenoid structures after applying more positive voltages up to +1 V. Specifically, the positively doped species (*i.e.*, polaron and bipolaron) were located over geometric defects and formed quinoids. Therefore, the higher the positive voltage, the higher the amount of (bi)polaron, resulting in a change in the polymer chain to quinoidal.[35] With increasing oxidation, the chain structure changed from benzenoid to quinoid and also affected the pi-stacking of the polymer film. As the oxidation level of the polymer film increases, the overlap between pi-orbitals of adjacent PEDOT chains may be disrupted, and therefore charge transport might deteriorate. Raman spectroscopy was also used to further characterize 2D-PEDOT films (Figure 3c). Strong bands *ca.* 1410 cm^{-1} (related to C═C symmetric) and *ca.* 1510 cm^{-1} (associated with C═C asymmetric) shifted at more positive voltages due to an increase in the number of doped species

https://doi.org/10.1021/acsapm.2c00899
ACS Appl. Polym. Mater. 2022, 4, 6978−6984

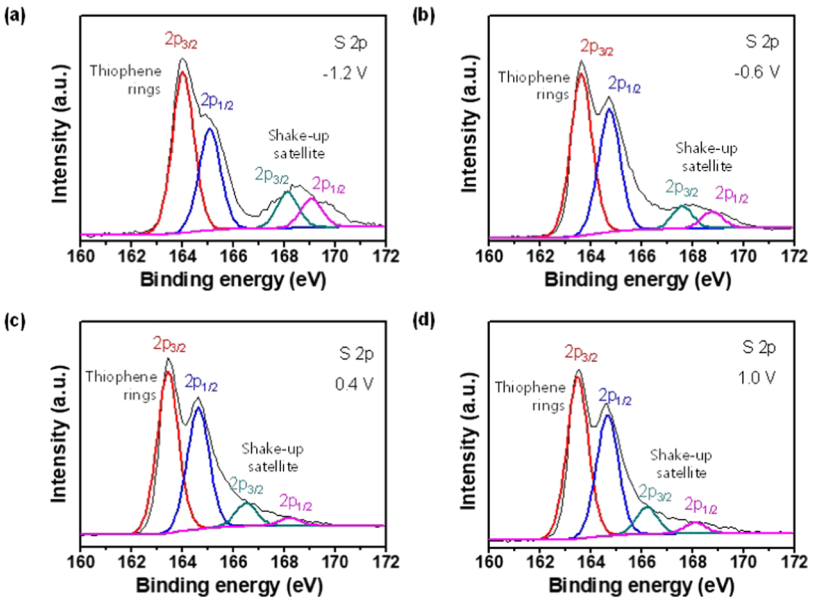

Figure 4. S 2p X-ray photoelectron spectra (XPS) of 2D-PEDOT with different applied potentials: (a) −1.2 V; (b) −0.6 V; (c) 0.4 V; and (d) 1.0 V.

(polaron or bipolaron) in the polymer chain. Raman spectra, therefore, also illustrated the changing proportion of (bi)-polarons in the polymer chains through the use of constant voltage charging systems.

The chemical compositions of 2D-PEDOT films were analyzed using X-ray photoelectron spectroscopy (XPS) (Figure 4). In the S 2p region of the charged 2D-PEDOT chains with different applied voltages, the peak width of signals increased with enhancing charge (*i.e.*, more positive voltage), with the other peak intensity at high-binding energy (*ca.* 170 eV) simultaneously diminishing. This change in signals might be due to a change in the valance band structure and shake-up phenomena of polymer chains with various oxidation values. In particular, the peak intensity of the shake-up satellite of the polymer films decreased with enhanced oxidation levels. At low oxidation levels (*i.e.*, neutral), the transition of valence electrons across the empty bandgap created a distinct structure in terms of the high-binding energy of the main S 2p peak.[36] On the other hand, the transition can be used in an activated state and is available in the bandgap for high oxidation levels (*i.e.*, polarons or bipolarons).[37] As a result, increasing oxidation levels in polymer films can decrease the shake-up satellite peak and generate a tail on the high-binding energy side to cause the broadening of the S 2p signal.

Optical Property Changes of the 2D-PEDOT Chain. UV−vis−near-infrared (NIR) spectra offer a qualitative evaluation of the neutral and charge carrier concentration of the polymer chain; therefore, it was used to investigate the types and transitions of carriers with different oxidation levels. As shown in Figure 5a, the polymer film at −1.0 V displayed a broad band in the visible (400−600 nm) and *ca.* 850 nm regions due to less oxidization of the polymer chain. On the other hand, as more polymer films were charged from −0.6 to +0.2 V, the IR background continued to increase, and polaronic transition became more pronounced at 1400 nm or more, while an absorption reduction was observed in the visible (400−600 nm) and *ca.* 850 nm areas. These spectra changes illustrate that PEDOT derivative films at more positive potentials will undergo oxidation such that the electron

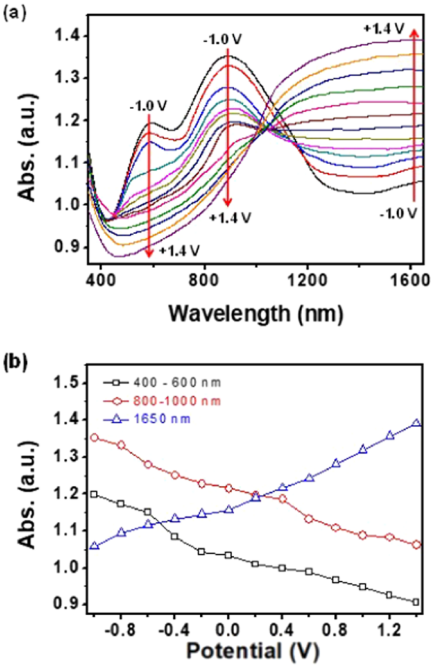

Figure 5. (a) UV−vis−NIR absorption of 2D-PEDOT with various applied potentials (voltage was applied at intervals of 0.2 V from −1.4 to +1.4 V). (b) Normalized absorption of 2D-PEDOT with the change of the chemical state in different wavelength ranges: visible (400−600 nm) and near-infrared (800−1000/1650 nm).

transfer to the polymer film transforms the neutral structure to polarons.[38] Moreover, higher oxidation levels (from +0.2 V) can increase the intensity of the band above 1400 nm and decrease bands in the visible (400−600 nm) and *ca.* 850 nm regions because the carrier type changes from polarons to bipolarons.[39] Absorption results of the polymer film in different wavelength ranges (400−600, 800−1000, and 1650 nm) are shown in Figure 5b. The absorption continuously decreased at low wavelength bands (visible (400−600 nm) and 800−1000 nm) but consistently increased around the NIR

https://doi.org/10.1021/acsapm.2c00899
ACS Appl. Polym. Mater. 2022, 4, 6978−6984

range (1650 nm). In particular, the intensity of the visible region (400−600 nm) displays two rapid dropwise regions (from −0.6 to −0.4 V and from 0 to +0.2 V) because of carrier changes from neutral to polarons and from polarons to bipolarons.[40,41]

Thermoelectric Property Changes of the 2D-PEDOT Chain. The substrate used in this work was an ITO-coated PET film. Once PEDOT derivative films are grown on the ITO substrate, the electrical conductivity of the polymer films would be higher than originally. To solve this problem, successful transfer of the polymer films from a conductive substrate (ITO/PET) to an insulating substrate (glass) was performed using adhesive polymer (epoxy resin) (Figure S5).[42]

To evaluate the material's thermoelectric characteristics, four-probe in-plane electrical conductivity, Seebeck coefficient, electrochemical carrier density, and carrier mobility of the polymer films were measured at room temperature. Figure 6a shows the electrical conductivities of films with different oxidation levels (from −1.4 to +1.4 V). When the positive potential was increased, the carrier density of the polymer chain was improved from 0.7×10^{20} to 4.24×10^{21} (Figure 6b). Thus, the electrical conductivity increased as the oxidation level increased. In particular, as the charge transport property changed from neutral to polarons (from −0.8 to −0.6 V) and from polarons to bipolarons (−0.2 to 0 V), the electrical conductivity increased rapidly. Electrical conductivity reached a peak value of 229.5 S cm^{-1} at an applied potential of +0.6 V (Figure 6a, inset). On the other hand, high applied potentials (from +1.2 V) overoxidized the polymer films, which caused a rapid diminution of the electrical conductivity (to 1.3×10^{-3} S cm^{-1} at 1.4 V) in spite of an abundance of charge carriers.[43] In addition, the morphology of the film at an overoxidized state suggested a different explanation. Namely, grains on the surface of the film collapse, and polymers suspended from the surface become agglomerated so that a two-dimensional planar structure is no longer formed (Figure S6). Moreover, carrier mobility originating from electrical conductivity and calculated carrier density ($\sigma = \mu eN$, where μ is the carrier mobility, e is the electron or hole charge, and N is the carrier density from charge current) suggests enhancement up to +1.0 V potentials and rapid diminishment from +1.2 V, respectively, because of the improvement of the electrical conductivity with higher carrier density and destruction of the polymer chains when overoxidized (Figure S7a). The Seebeck coefficient (S) is a criterion that illustrates the basic electronic movement ability of a material. It stands on the entropy of a carrier with a unit charge. The Seebeck coefficient presents a contrasting aspect to the electrical conductivity, which is inversely proportional to the carrier density (Figure 6c). The Seebeck coefficient displayed the highest value at −1.4 V (156.3 μV K^{-1}) and the lowest value at 0.6 V (55.12 μV K^{-1}). Consequently, the power factor (PF = σS^2) of the films suggested 72.6 μW m^{-1} K^{-2} as the highest value at +0.6 V and 1.3×10^{-3} μW m^{-1} K^{-2} as the lowest value at +1.4 V (Figure S7b). In addition, to confirm the stability of the 2D-PEDOT film with adjusted oxidation states, thermoelectric performance factors (σ and S) according to a time interval of 4 weeks were compared. As shown in Figure S8, there is little change in the value of the performance factors over time. Therefore, the 2D-PEDOT film subjected to a chemical oxidation change maintains a constant state without a state change over time.

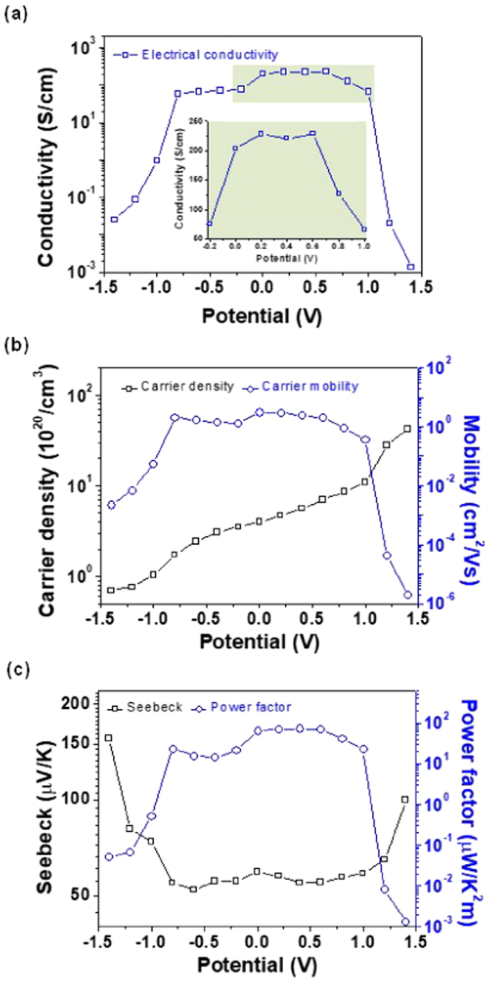

Figure 6. (a) Electrical conductivity, (b) carrier density and carrier mobility, and (c) Seebeck coefficient and power factor of 2D-PEDOT films with applied voltage variations.

CONCLUSIONS

In summary, we evaluated the thermoelectric properties of 2D-PEDOT films using controlled electrochemical oxidation levels. These polymer films exhibited enhanced electrochemical charge transport at more positive potentials because these positive potentials generated charge transfer (hole) in the polymer chains. The value of the carrier density in the polymer chains changed from 0.7×10^{20} at −1.4 V to 4.24×10^{21} at +1.4 V potential. Thermoelectric properties such as electrical conductivity, carrier mobility, and Seebeck coefficient were then exactly controlled using various applied potentials. Consequently, the power factor of the 2D-PEDOT film displayed a maximum value of 72.6 μW m^{-1} K^{-2} at +0.6 V, which was much higher than that achieved in a neutral state (5.1×10^{-2} μW m^{-1} K^{-2}) or with an overoxidized state (1.3×10^{-3} μW m^{-1} K^{-2}). The results reported here indicate that simple electrochemical oxidation level control could be used to modify the thermoelectric properties of other conductive organic materials.

MATERIALS AND METHODS

Materials. 3,4-ethylenedioxythiophene (EDOT), 1,3,5-tri(2-thienyl)-benzene (TTB), tetrabutylammonium perchlorate, and propylene

https://doi.org/10.1021/acsapm.2c00899
ACS Appl. Polym. Mater. 2022, 4, 6978−6984

carbonate were purchased from Aldrich Chemical Co. and used without further purification.

Synthesis of 2D-PEDOT Chains. Prior to synthesis, an ITO-coated PET film was cleaned with acetone, isopropyl alcohol (IPA), and distilled water in sequence. The cleaned ITO-coated PET film was immersed in an electrolyte solution that contained propylene carbonate as a solvent, 0.1 M tetrabutylammonium perchlorate as a salt, and 10 mM EDOT and 0.5 mM TTB as monomers. The electropolymerization was conducted at room temperature over a voltage range of −1.0 to +1.4 V (*vs* saturated calomel electrode (SCE)) using 100 mV s^{-1} of scan rate for 10 cycles. The electropolymerization process was conducted with an SP-200 potentiostat (Biologic). 2D-PEDOT decorated-PET films were then removed, carefully washed with isopropyl alcohol (IPA), and dried at 60 °C for 2 h.

Chemical State Changes of 2D-PEDOT Chains. The chemical state of the 2D-PEDOT film was controlled using an electrochemical process. All electrochemical processing was conducted with an SP-200 potentiostat (Biologic). In detail, 2D-PEDOT films were placed in an electrochemical cell consisting of a counter electrode (platinum wire), a reference electrode (Ag/AgCl), and an electrolyte (0.1 M tetrabutylammonium perchlorate in the propylene carbonate). 2D-PEDOT films were then held at different set potentials (−1.4 to 1.4 V *vs* SCE) for 3 min. Films were then washed with IPA and dried at 60 °C for 3 h in a nitrogen atmosphere.

Characterizations. A Hitachi S-2700 was used to obtain field-emission scanning electron microscopy (FE-SEM) images. Fourier-transform infrared (FTIR) and Raman spectra were measured using an IRTracer-100 (Shimadzu) and LabRam HR Evo confocal Raman (Horiba, 785 nm), respectively. UV−vis−NIR spectra were collected on a UV-3600 Plus spectrophotometer (Shimadzu). X-ray photoelectron spectroscopy (XPS) was performed using an Axis Nova (Kratos).

Thermoelectric Coefficients Measurement of 2D-PEDOT Films. To measure thermoelectric coefficients, PEDOT derivative films were transferred from the conductive substrate (ITO/PET) to the insulating substrate (epoxy/glass). In detail, insulating epoxy adhesive (Epoxies, #20-3302) coated glass substrates were placed on PEDOT derivative film surfaces and cured at room temperature for 6 h. The ITO/PET substrate was then peeled away from the film surface to form PEDOT/epoxy multilayers on the glass substrate. For thermoelectric measurements, contacts were made to samples after a transfer process using thermal evaporation of gold through a shadow mask (Al).

The electrical conductivity of the film was measured using a four-point probe with a Keithley 2400 source-meter unit. The electrical conductivity (σ, S cm^{-1}) of the film was calculated using the following equation $\sigma = L/(R{\cdot}A)$, where L is the film thickness (cm), R is the film resistance (Ω), and A is the cross-sectional area (cm^2) of the film between contact parts. The Seebeck factor (S) measurement was performed using a custom setting in which two tungsten tips (Keithley 2700) and two thermocouple probes (Fluke 1529) were used for measuring voltage (V) and temperature (T). Among device components, a Peltier element 10 mm away provided a temperature difference ($\Delta T = T_H - T_C$). Measurements were made with a ΔT of about 300 ± 3 K.

■ ASSOCIATED CONTENT

Supporting Information

The Supporting Information is available free of charge at https://pubs.acs.org/doi/10.1021/acsapm.2c00899.

Synthesis of the polymers; EIS of polymer films with different TTB amounts; CV curves of PEDOT and polymerized TTB; crystallinity comparison of the polymer film; film transfer; FE-SEM images of 2D-PEDOT films with different chemical states; thermoelectric factor values in a limited voltage range; and stability of the polymer films (PDF)

■ AUTHOR INFORMATION

Corresponding Author

Shrayesh N. Patel − *Pritzker School of Molecular Engineering, University of Chicago, Chicago, Illinois 60637, United states;* orcid.org/0000-0003-3657-827X; Phone: +1-773-702-7717; Email: shrayesh@uchicago.edu

Author

Jun Seop Lee − *Department of Materials Science and Engineering, Gachon University, Seongnam-Si, Gyeonggi-Do 13120, Republic of Korea;* orcid.org/0000-0002-7350-2875

Complete contact information is available at: https://pubs.acs.org/10.1021/acsapm.2c00899

Notes

The authors declare no competing financial interest.

■ ACKNOWLEDGMENTS

This work made use of the shared facilities at the University of Chicago Materials Research Science and Engineering Center, supported by National Science Foundation under award number DMR-2011854. Parts of this work were carried out at the Soft Matter Characterization Facility of the University of Chicago. (J. S. Lee) This work was supported by the National Research Foundation of Korea (NRF) grant funded by the Korean government (MSIT) (nos. 2020R1A4A407983711).

■ REFERENCES

(1) Jung, J.; Suh, E. H.; Jeong, Y.; Yun, D.-J.; Park, S. C.; Oh, J. G.; Jang, J. Ionic-Liquid Doping of Carbon Nanotubes with [HMIM]-[BF_4] for Flexible Thermoelectric Generators. *Chem. Eng. J.* **2022**, *438*, No. 135526.

(2) Bubnova, O.; Crispin, X. Towards Polymer-Based Organic Thermoelectric Generators. *Energy Environ. Sci.* **2012**, *5*, 9345−9362.

(3) Wang, K.; Hou, C.; Zhang, Q.; Li, Y.; Wang, H. Highly Integrated Fiber-Shaped Thermoelectric Generators with Radially Heterogeneous Interlayers. *Nano Energy* **2022**, *95*, No. 107055.

(4) Jeong, M. H.; Kim, K.-C.; Kim, J.-S.; Choi, K. J. Operation of Wearable Thermoelectric Generators Using Dual Sources of Heat and Light. *Adv. Sci.* **2022**, *9*, No. 2104915.

(5) Kim, G.-H.; Shao, L.; Zhang, K.; Pipe, K. P. Engineered Doping of Organic Semiconductors for Enhanced Thermoelectric Efficiency. *Nat. Mater.* **2013**, *12*, 719−723.

(6) Zaia, E. W.; Sahu, A.; Zhou, P.; Gordon, M. P.; Foster, J. D.; Aloni, S.; Liu, Y.-S.; Gou, J.; Urban, J. J. Carrier Scattering at Alloy Nanointerfaces Enhances Power Factor in PEDOT:PSS Hybrid Thermoelectrics. *Nano Lett.* **2016**, *16*, 3352−3359.

(7) Liang, L.; Wang, M.; Wang, X.; Peng, P.; Liu, Z.; Chen, G.; Sun, G. Initiating a Stretchable, Compressible, and Wearable Thermoelectric Generator by a Spiral Architecture with Ternary Nanocomposites for Efficient Heat Harvesting. *Adv. Funct. Mater.* **2022**, *32*, No. 211435.

(8) Rincón-García, L.; Ismael, A. K.; Evangeli, C.; Grace, I.; Rubio-Bollinger, G.; Porfyraskis, K.; Agrait, N.; Lambert, C. J. Molecular Design and Control of Fullerene-Based Bi-Thermoelectric Materials. *Nat. Mater.* **2016**, *15*, 289−294.

(9) Ail, U.; Jafari, M. J.; Wang, H.; Ederth, T.; Berggren, M.; Crispin, X. Thermoelectric Properties of Polymeric Mixed Conductors. *Adv. Funct. Mater.* **2016**, *26*, 6288−6296.

(10) Kim, H.-J.; Kim, S. M.; Lee, S.; Sung, S.-K.; Min, J.-W.; Lim, K.-H.; Lee, T. K.; Song, H.-E.; Kim, Y.; Kim, J.; Lee, Y. Rapid Evaluation System for Photovoltaic Cell and Thermoelectric Generator Hybrid Devices Depending on Temperature via Transparent Heater. *ACS Appl. Energy Mater.* **2022**, *5*, 2669−2674.

(11) Yu, Y.; Guo, Z.; Zhu, W.; Zhou, J.; Guo, S.; Wang, Y.; Deng, Y. High-Integration and High-Performance Micro Thermoelectric Generator by Femtosecond Laser Direct Writing for Self-Powered IoT Devices. *Nano Energy* **2022**, *93*, No. 106818.
(12) Perumal, S.; Bellare, P.; Shenoy, U. S.; Waghmare, U. V.; Biswas, K. Low Thermal Conductivity and High Thermoelectric Performance in Sb and Bi Codoped GeTe: Complementary Effect of Band Convergence and Nanostructuring. *Chem. Mater.* **2017**, *29*, 10426−10435.
(13) Liu, W.; Sun, S.; Zhu, X. Organic Photovoltaics Integrated with Thermoelectric Generator Achieving Low Critical Temperature Difference and Efficient Energy Conversion. *Adv. Funct. Mater.* **2022**, *32*, No. 2109410.
(14) Dörling, B.; Ryan, J. D.; Craddock, J. D.; Sorrentino, A.; Basaty, A. E.; Gomez, A.; Garriga, M.; Pereiro, E.; Anthony, J. E.; Weisenberger, M. C.; Goni, A. R.; Muller, C.; Campoy-Quiles, M. Photoinduced p- to n-type Switching in Thermoelectric Polymer-Carbon Nanotube Composites. *Adv. Mater.* **2016**, *28*, 2782−2789.
(15) Suarez, F.; Nozariasbmarz, A.; Vashee, D.; Ozturk, M. C. Designing Thermoelectric Generators for Self-Powered Wearable Electronics. *Energy Environ. Sci.* **2016**, *9*, 2099−2113.
(16) Nayak, R.; Shetty, P.; Selvakumar, M.; Rao, A.; Rao, K. M. Formulation of New Screen Printable PANI and PANI/Graphite Based Inks: Printing and Characterization of Flexible Thermoelectric Generators. *Energy* **2022**, *238*, No. 121680.
(17) Kim, J. Y.; Grossman, J. C. Optimization of the Thermoelectric Figure of Merit in Crystalline C_{60} with Intercalation Chemistry. *Nano Lett.* **2016**, *16*, 4203−4209.
(18) Tu, S.; Tian, T.; Oechsle, A. L.; Yin, S.; Jiang, X.; Cao, W.; Li, N.; Scheel, M. A.; Reb, L. K.; Hou, S.; Bandarenka, A. S.; Schwartzkopf, M.; Roth, S. V.; Müller-Buschbaum, P. Improvement of the Thermoelectric Properties of PEDOT:PSS Films via DMSO Addition and DMSO/Salt Post-Treatment Resolved from a Fundamental View. *Chem. Eng. J.* **2022**, *429*, No. 132295.
(19) Wei, S.; Zhang, Y.; Lv, H.; Deng, L.; Chen, G. SWCNT Network Evolution of PEDOT:PSS/SWCNT Composites for Thermoelectric Application. *Chem. Eng. J.* **2022**, *428*, No. 131137.
(20) Chen, G.; Xu, W.; Zhu, D. Recent Advances in Organic Polymer Thermoelectric Composites. *J. Mater. Chem. C* **2017**, *5*, 4350−4360.
(21) Zhang, H.; Koo, J.; Xu, C.; Sretenovic, M.; Yan, B.; Ke, X. Exchange-Biased Topological Transverse Thermoelectric Effects in a Kagome Ferrimagnet. *Nat. Commun.* **2022**, *13*, No. 1091.
(22) Yan, H.; Sada, N.; Toshima, N. Thermal Transporting Properties of Electrically Conductive Polyaniline Films as Organic Thermoelectric Materials. *J. Therm. Anal. Calorim.* **2002**, *69*, 881−887.
(23) Feng-Xing, J.; Xu, J.-K.; Lu, B.-Y.; Xie, Y.; Huang, R.-J.; Li, L.-F. Thermoelectric Performance of Poly(3,4- ethylenedioxythiophene): Poly(styrenesulfonate). *Chin. Phys. Lett.* **2008**, *25*, 2202.
(24) Moses, D.; Denenstein, A. Experimental Determination of the Thermal Conductivity of a Conducting Polymer: Pure and Heavily Doped Polyacetylene. *Phys. Rev. B* **1984**, *30*, 2090−2097.
(25) Snyder, G. J.; Toberer, E. S. Complex Thermoelectric Materials. *Nat. Mater.* **2008**, *7*, 105−114.
(26) Shelimova, L. E.; Karpinskii, O. G.; Konstantinov, P. P.; Avilov, E. S.; Kretova, M. A.; Zemskov, V. S. Crystal Structures and Thermoelectric Properties of Layered Compounds in the ATe−Bi_2Te_3 (A = Ge, Sn, Pb) Systems. *Inorg. Mater.* **2004**, *40*, 451−460.
(27) Liu, Z.; Gao, W.; Oshima, H.; Nagase, K.; Lee, C.-H.; Mori, T. Maximizing the Performance of n-type Mg_3Bi_2 Based Materials for Room-Temperature Power Generation and Thermoelectric Cooling. *Nat. Commun.* **2022**, *13*, No. 1120.
(28) Khan, Z. U.; Brooke, R.; Liu, X.; Gabrielsson, R.; Ederth, T.; Evans, D. R.; Andreasen, J. W.; Fahlman, M.; Crispin, X.; et al. Acido-Basic Control of the Thermoelectric Properties of Poly(3,4-ethylenedioxythiophene)tosylate (PEDOT-Tos) Thin Films. *J. Mater. Chem. C* **2015**, *3*, 10616−10623.
(29) Fontana, M. T.; Stanfield, D. A.; Scholes, D. T.; Winchell, K. J.; Tolbert, S. H.; Schwartz, B. J. Evaporation vs Solution Sequential Doping of Conjugated Polymers: F_4TCNQ Doping of Micrometer-Thick P3HT Films for Thermoelectrics. *J. Phys. Chem. C* **2019**, *123*, 22711−22727.
(30) Jacobs, I. E.; Lin, Y.; Huang, Y.; Ren, X.; Simatos, D.; Chen, C.; Tjhe, D.; Statz, M.; Lai, L.; Finn, P. A.; et al. High-Efficiency Ion-Exchange Doping of Conducting Polymers. *Adv. Mater.* **2022**, *34*, No. 2102988.
(31) Hofmann, A. I.; Kroon, R.; Yu, L.; Muller, C. Highly Stable Doping of a Polar Polythiophene Through Co-Processing with Sulfonic Acids and Bistriflimide. *J. Mater. Chem. C* **2018**, *6*, 6905−6910.
(32) Jacobs, I. E.; Aasen, E. W.; Oliveira, J. L.; Fonseca, T. N.; Roehling, J. D.; Li, J.; Zhang, G.; Augustine, M. P.; Mascal, M.; Moule, A. J. Comparison of Solution-Mixed and Sequentially Processed P3HT:F4TCNQ Films: Effect of Doping-Induced Aggregation on Film Morphology. *J. Mater. Chem. C* **2016**, *4*, 3454−3466.
(33) Patel, S. N.; Glaudell, A. M.; Kiefer, D.; Chabinyc, M. L. Increasing the Thermoelectric Power Factor of a Semiconducting Polymer by Doping from the Vapor Phase. *ACS Macro Lett.* **2016**, *5*, 268−272.
(34) Park, T.; Park, C.; Kim, B.; Shin, H.; Kim, E. Flexible PEDOT Electrodes with Large Thermoelectric Power Factors to Generate Electricity by the Touch of Fingertips. *Energy Environ. Sci.* **2013**, *6*, 788−792.
(35) Zhu, B.; Bryant, D. T.; Akbarinejad, A.; Travas-Sejdic, J.; Pilkington, L. I. A Novel Electrochemical Conducting Polymer Sensor for the Rapid, Selective and Sensitive Detection of Biothiols. *Polym. Chem.* **2022**, *13*, 508−516.
(36) Ouyang, J.; Xu, Q.; Chu, C.-W.; Yang, Y.; Li, G.; Shinar, J. On the Mechanism of Conductivity Enhancement in Poly(3,4-ethylenedioxythiophene):Poly(styrene sulfonate) Film Through Solvent Treatment. *Polymer* **2004**, *45*, 8443−8450.
(37) Morea, G.; Sabbatini, L.; West, R. H.; Vickerman, J. C. Surface Characterization (XPS and SIMS) of Emersed Polybithiophene Electrodes. *Surf. Interface Anal.* **1992**, *18*, 421−429.
(38) Bezgin, B.; Yagan, A.; Onal, A. M. Electrochemical Co-Polymerization of a Novel Fluorene Derivative with 3,4-Ethylenedioxythiophene. *J. Electroanal. Chem.* **2009**, *632*, 143−148.
(39) Zhao, J.; Tan, D.; Chen, G. A Strategy to Improve the Thermoelectric Performance of Conducting Polymer Nanostructures. *J. Mater. Chem. C* **2017**, *5*, 47−53.
(40) Petsagkourakis, I.; Pavlopoulou, E.; Portale, G.; Kuropatwa, B. A.; Dilhaire, S.; Fleury, G.; Hadziioannou, G. Structurally-Driven Enhancement of Thermoelectric Properties within Poly(3,4-ethylenedioxythiophene) Thin Films. *Sci. Rep.* **2016**, *6*, No. 30501.
(41) Shi, W.; Zhao, T.; Xi, J.; Wang, D.; Shuai, Z. Unravelling Doping Effects on PEDOT at the Molecular Level: From Geometry to Thermoelectric Transport Properties. *J. Am. Chem. Soc.* **2015**, *137*, 12929−12938.
(42) Thomas, M. A.; Cui, J. B. Highly Uniform 2D Growth, Substrate Transfer, and Electrical Characterization of Electrodeposited ZnO Thin Films. *J. Electrochem. Soc.* **2013**, *160*, D218−D225.
(43) Bouabdallaoui, M.; Aouzal, Z.; Jadi, S. B.; Jaouhari, A. E.; Bazzaoui, M.; Levi, G.; Aubard, J.; Bazzaoui, E. A. X-ray Photoelectron and in situ and ex situ Resonance Raman Spectroscopic Investigations of Polythiophene Overoxidation. *J. Solid State Electrochem.* **2017**, *21*, 3519−3532.

https://doi.org/10.1021/acsapm.2c00899
ACS Appl. Polym. Mater. 2022, 4, 6978−6984